LETTERS

A novel pathway regulates memory and plasticity via SIRT1 and miR-134

Jun Gao[1,2,3]*, Wen-Yuan Wang[1,2]*, Ying-Wei Mao[1,2], Johannes Gräff[1,4], Ji-Song Guan[1,2], Ling Pan[1,2], Gloria Mak[1,2], Dohoon Kim[1,2]†, Susan C. Su[1,2] & Li-Huei Tsai[1,2,4]

The NAD-dependent deacetylase Sir2 was initially identified as a mediator of replicative lifespan in budding yeast and was subsequently shown to modulate longevity in worms and flies[1,2]. Its mammalian homologue, SIRT1, seems to have evolved complex systemic roles in cardiac function, DNA repair and genomic stability. Recent studies suggest a functional relevance of SIRT1 in normal brain physiology and neurological disorders. However, it is unknown if SIRT1 has a role in higher-order brain functions. We report that SIRT1 modulates synaptic plasticity and memory formation via a microRNA-mediated mechanism. Activation of SIRT1 enhances, whereas its loss-of-function impairs, synaptic plasticity. Surprisingly, these effects were mediated via post-transcriptional regulation of cAMP response binding protein (CREB) expression by a brain-specific microRNA, miR-134. SIRT1 normally functions to limit expression of miR-134 via a repressor complex containing the transcription factor YY1, and unchecked miR-134 expression following SIRT1 deficiency results in the downregulated expression of CREB and brain-derived neurotrophic factor (BDNF), thereby impairing synaptic plasticity. These findings demonstrate a new role for SIRT1 in cognition and a previously unknown microRNA-based mechanism by which SIRT1 regulates these processes. Furthermore, these results describe a separate branch of SIRT1 signalling, in which SIRT1 has a direct role in regulating normal brain function in a manner that is disparate from its cell survival functions, demonstrating its value as a potential therapeutic target for the treatment of central nervous system disorders.

The mammalian Sir2 homologue SIRT1 is involved in a variety of complex processes relevant to ageing, including the regulation of oxidative stress, metabolism control and circadian rhythms[1–4]. We demonstrated previously that SIRT1 gain-of-function is neuroprotective in overactive Cdk5 and mutant superoxide dismutase models of neurodegeneration, which are relevant to Alzheimer's disease and ALS, respectively[5]. Moreover, SIRT1 has recently been implicated in molecular pathways regulated by cocaine[6], suggesting that, in addition to its involvement in neurogenesis and neuroprotection, SIRT1 has further functions in the brain that are yet to be described.

To evaluate directly the physiological role of SIRT1 in learning and memory, mutant mice lacking SIRT1 catalytic activity in a brain-specific manner (SIRT1Δ) were generated by crossing mice carrying a floxed *SIRT1*$^{\Delta ex4}$ allele[7,8] with *Nestin-Cre* transgenic mice. In tests of associative memory, SIRT1Δ mice showed a significant decrease in freezing behaviour as evaluated by both contextual (Fig. 1a) and tone-dependent (Supplementary Fig. 2a) fear-conditioning paradigms. Shock sensitivity and locomotor activity did not differ between SIRT1Δ mice and littermate controls (Fig. 1b, Supplementary Fig. 2b). SIRT1Δ mice showed a similarly decreased memory performance in a novel object recognition task (Fig. 1c), which relies on the hippocampus and cortex[9]. The time spent exploring the objects during training did not significantly differ between groups (Fig. 1d). In the Morris water maze, SIRT1Δ mice displayed significantly increased escape latencies in the hidden platform paradigm (Fig. 1e), while spending less time in the target quadrant in a probe trial (Fig. 1f) compared with control mice, indicating that SIRT1 has a role in spatial learning. Visual function and swimming ability were not affected in the SIRT1Δ mice (Supplementary Fig. 2c, d). Together, these results show that SIRT1 has an important role in several forms of memory.

Next, we used a long-term potentiation (LTP) paradigm to determine directly the role of SIRT1 in synaptic plasticity. LTP in hippocampal CA1 neurons, induced by two θ burst (2 × TBS) stimulation of the Schaffer collaterals in control mice, was abrogated in SIRT1Δ mice, demonstrating a requirement of SIRT1 in synaptic plasticity (Fig. 1g). CA1 neurons in SIRT1Δ mice had normal basal synaptic transmission (Supplementary Fig. 3a, b) compared to control mice. These results demonstrate that the LTP deficits caused by SIRT1 inactivation are not due to impaired synaptic transmission.

The brains of SIRT1Δ mice had a grossly normal anatomy (data not shown). However, experiments using an antibody against synaptophysin (SVP), which labels the presynaptic terminals of functional synapses[10], revealed significant decreases in SVP immunoreactivity in the hippocampal striatum radiatum of SIRT1Δ mice, as well as reduced SVP protein content in the SIRT1Δ hippocampus, compared to controls (Fig. 1h and i). Golgi impregnation demonstrated that the dendritic spine density of CA1 pyramidal neurons is significantly decreased in the hippocampus of SIRT1Δ mice (Fig. 1j). These results indicate that SIRT1 regulates synapse formation, synaptic plasticity, and memory formation.

BDNF and *CREB* are two genes that have critical roles in synaptic plasticity and modulating synapse formation[11–13]. Both mRNA and protein levels of BDNF were significantly decreased in SIRT1Δ hippocampi compared with controls (Fig. 2a). CREB binds to several *BDNF* promoters and plays a key role in the activity-dependent regulation of BDNF expression[14–17]. We performed chromatin immunoprecipitation (ChIP) to further examine the association of CREB and *BDNF* promoters. Baseline binding of CREB to *BDNF* promoters 1, 2, and 4 was reduced in the SIRT1Δ hippocampus (Fig. 2b). As reported previously[15,17], binding of CREB to *BDNF* promoters 1 and 4 was increased after contextual fear conditioning training. In SIRT1Δ mice, however, this training-related increase in *BDNF* promoter 1 and 4 binding by CREB was abolished (Supplementary Fig. 4a).

[1]Picower Institute for Learning and Memory, Department of Brain and Cognitive Sciences, Massachusetts Institute of Technology, Cambridge, Massachusetts 02139, USA. [2]Howard Hughes Medical Institute, Massachusetts Institute of Technology, Cambridge, Massachusetts 02139, USA. [3]Model Animal Research Center, MOE Key Laboratory of Model Animal for Disease Study, Nanjing University, Nanjing 210061, China. [4]Stanley Center for Psychiatric Research, Broad Institute, Cambridge, Massachusetts 02142, USA. †Present address: Whitehead Institute for Biomedical Research, Cambridge, Massachusetts 02142, USA.
*These authors contributed equally to this work.

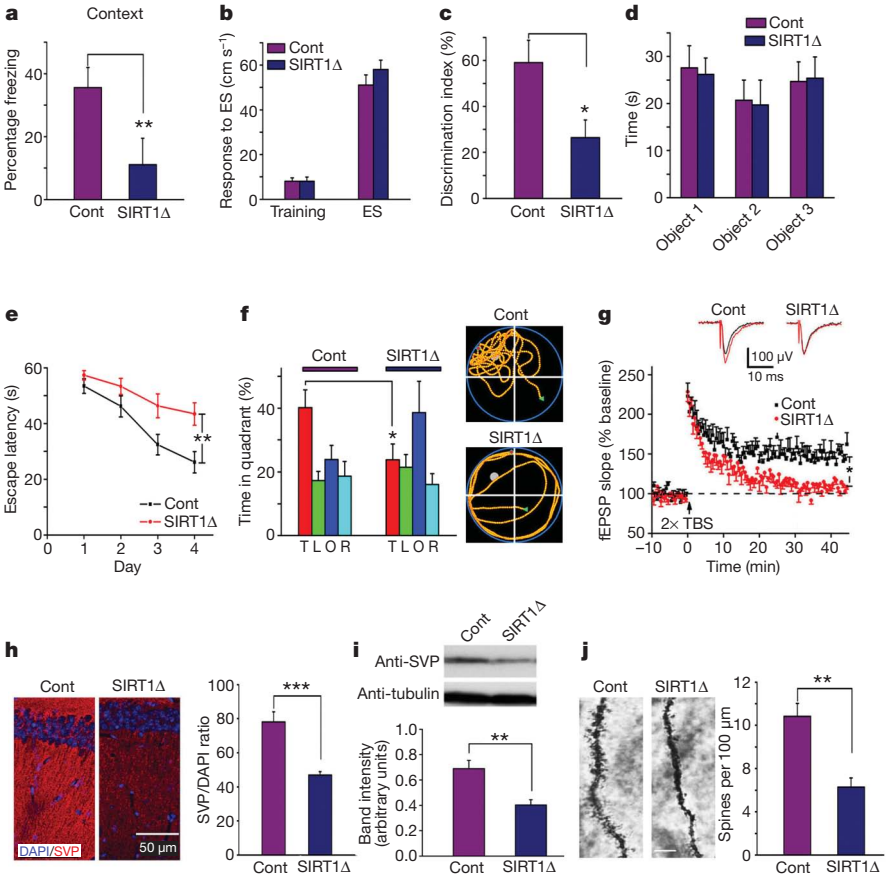

Figure 1 | SIRT1 loss-of-function impairs memory and synaptic plasticity. **a**, Freezing time of SIRT1Δ mice and littermate controls (Cont) 24 h after contextual fear conditioning training. **b**, Shock sensitivities did not differ between control and SIRT1Δ mice. ES, electrical stimulation. **c**, SIRT1Δ and control mice were tested for novel object discrimination 24 h after training. **d**, Pre-test exploration times were equal for each object. **e**, Escape latencies of SIRT1Δ and control mice were examined with the Morris water maze hidden platform test. **f**, Left panel, swimming time spent in each quadrant in the probe trial on day 5 (T, target; L, left; O, opposite; R, right). Right panel, representative path tracings of the probe test. **g**, LTP measurements were performed in the CA1 region of acute slices from SIRT1Δ mice and controls. fEPSP, field excitatory postsynaptic potentials. **h**, SVP immunoreactivity in SIRT1Δ and control hippocampi. **i**, Western blots from hippocampal lysates examined SVP in SIRT1Δ and control mice. **j**, Density of Golgi-impregnated hippocampal neuronal dendritic spines was measured in SIRT1Δ and control mice. TBS, theta-burst stimulation; SVP, synaptophysin; SVP/DAPI ratio, ratio of SVP (rhodamine, A_{548}) over DAPI (A_{490}). $^{*}P < 0.05$, $^{**}P < 0.01$, $^{***}P < 0.001$. All histograms represent average ± s.e.m.

One possible explanation for the decreased CREB binding to *BDNF* promoters observed in SIRT1Δ mice is that CREB itself is downregulated. Consistent with this notion, CREB protein levels were significantly reduced in SIRT1Δ hippocampi (Fig. 2c, left). Although overall CREB levels were reduced in the SIRT1Δ mice, CREB phosphorylation was still increased by fear conditioning training (Supplementary Fig. 4b). However, in contrast to BDNF, mRNA levels of *CREB* were not altered (Fig. 2c, right), indicating that CREB protein levels are downregulated in SIRT1Δ brains via post-transcriptional mechanisms.

To investigate such mechanisms, we considered a well-known means of post-transcriptional regulation of gene expression, the inhibition of translation via microRNA (miRNA). miRNAs are expressed at high levels in the brain[18,19], and the involvement of miRNA in numerous aspects of normal and abnormal brain function has been reported[19,20]. We compared the expression of miRNAs in SIRT1Δ hippocampi with littermate control hippocampi using a miRNA microarray (Exqion), and found that a number of brain-enriched miRNAs differed in expression between the two groups (Supplementary Fig. 5). We evaluated the expression of eight miRNAs that were significantly altered in the microarray analysis, including five upregulated and three downregulated miRNAs, using mature miRNA-specific quantitative PCR (qPCR). Consistent with the microarray, our qPCR analyses confirmed significant changes in expression of all eight miRNAs (Fig. 2d).

Of these miRNAs, miRNA-134 was of particular interest, as it is specifically expressed in the brain and has been demonstrated to negatively regulate dendritic spine formation *in vitro*[21]. Comparative genomic analyses of the 3′ untranslated region (3′UTR) of the mouse *CREB* gene revealed three partial complementary binding sites for miR-134, with one site being well-conserved (Supplementary Fig. 6a). To determine whether miR-134 binds directly to and inhibits the translation of *CREB* mRNA, we carried out a CREB activity luciferase (Luc) reporter assay in which luciferase is driven by a minimal promoter downstream of CREB-binding elements. Co-transfection of miR-134 with CRE-Luc resulted in a significant decrease in CREB activity in cultured CAD cells, a neural cell line (Fig. 2e). As a negative control, we created a miR-134 mutant containing mutations in the miR-134 seed region (mut-miR-134). Expression of mut-miR-134 did not affect CREB activity (Fig. 2e). The expression of miR-34b-5p or miR-34c, two other miRNAs upregulated in brains of SIRT1Δ mice, had no effect on CREB activity (Supplementary Fig. 6b), indicating specific regulation of CREB by miR-134. Finally, miR-134 loss-of-function using a locked-nucleic-acid (LNA)-modified oligonucleotide probe (LNA-miR-134), which achieves specific knockdown of endogenous miR-134, significantly enhanced CREB activity (Fig. 2e). These results indicate that miR-134 regulates CREB protein expression via a post-transcriptional mechanism.

To verify the direct nature of CREB inhibition by miR-134, we generated a luciferase reporter construct in which the 3′UTR of CREB, containing all three predicted miR-134 target sequences, was inserted downstream of a luciferase expression cassette (WT-CREB). As expected, co-expression of miR-134 with WT-CREB significantly attenuated reporter expression (Fig. 2f). A luciferase reporter construct linked to the 3′UTR of *CREB* containing multiple mutations within the three miR-134 target sequences (mut-CREB) was refractory to knockdown by miR-134 (Fig. 2f). Expression of mut-CREB alone resulted in a significant increase in luciferase activity, indicating a derepression of the reporter construct by endogenous miR-134 (Fig. 2f). These results indicate that miR-134 attenuates CREB expression via a specific interaction with the target regions within the 3′UTR of *CREB*. Moreover, overexpression of miR-134, but not mut-miR-134, in cultured CAD cells resulted in reduced levels of CREB protein relative to a scrambled miR control (Scr-miR; Fig. 2g). In contrast, delivery of LNA-miR-134 resulted in increased CREB protein levels compared to LNA-scrambled-miR

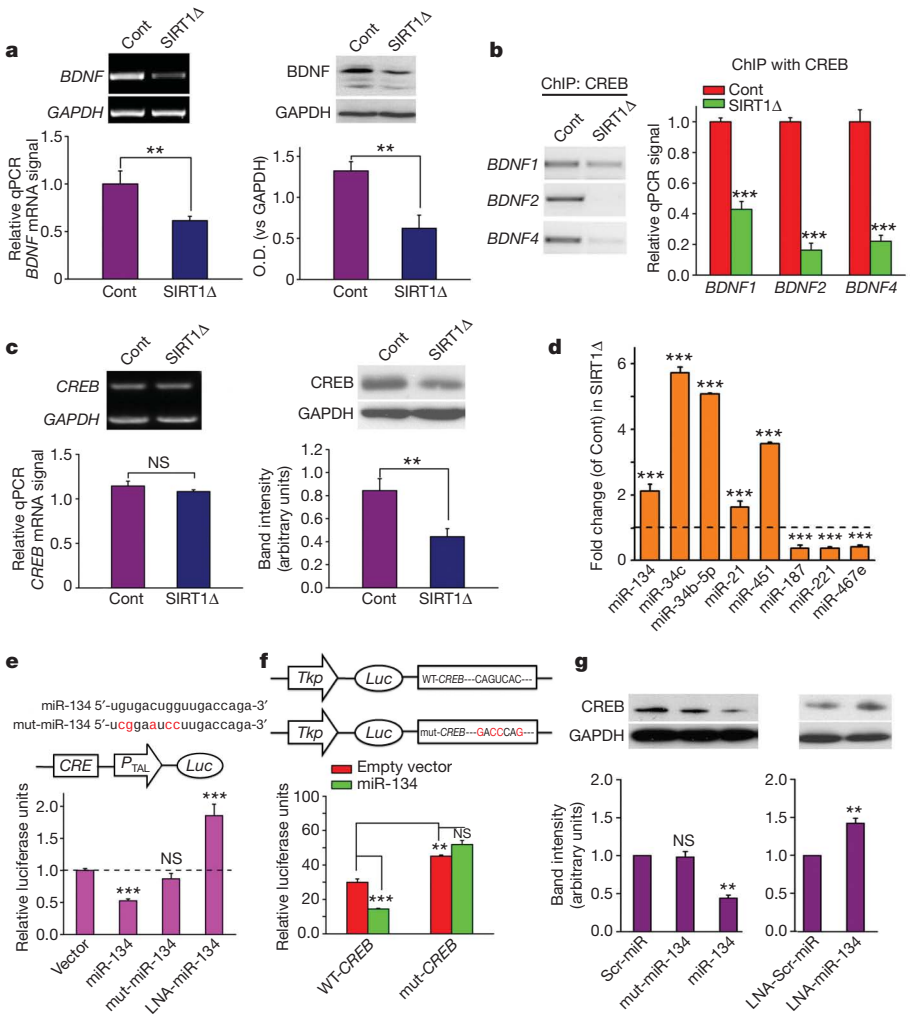

Figure 2 | BDNF and CREB are downregulated, whereas miRNA-134 is upregulated, in SIRT1Δ mice. **a**, BDNF in the SIRT1Δ and control mouse hippocampus. Left, mRNA levels; right, western blot. **b**, Chromatin immunoprecipitation (ChIP) with an anti-CREB antibody was followed by qPCR for *BDNF* promoters 1, 2 and 4. **c**, CREB in the SIRT1Δ and control mouse hippocampus. Left: mRNA levels; right, western blot. **d**, qPCR of selected miRNAs from hippocampi of SIRT1Δ and control mice. **e**, CAD cells were transfected with the plasmids or LNA indicated together with CRE-Luc. **f**, Luciferase reporter constructs containing either a wild-type (WT-CREB) or a mutated (mut-CREB) CREB 3′UTR region, were cotransfected with miR-134 or control. **g**, CREB protein expression in CAD cells after transfection with the indicated constructs or LNAs. Scr, scrambled; mut, mutant; LNA, locked-nucleic-acid (LNA); CRE-Luc, CREB activity reporter construct. $^{**}P < 0.01$; $^{***}P < 0.001$; NS, not significant.

(LNA-scr-miR) control (Fig. 2g), indicating that, under normal conditions, miR-134 has a limiting effect on CREB translation.

To investigate how SIRT1 modulates miR-134 transcription, we conducted ChIP with an anti-SIRT1 antibody and examined the association of SIRT1 with DNA sequences spanning ~5 kilobases upstream of the pre-miR-134 sequence. We found that two regions, R3 and R7, could be specifically amplified from SIRT1 ChIP, indicating that SIRT1 is associated with potential regulatory elements upstream of miR-134 (Fig. 3a). The specificity of the interaction was verified by ChIP analyses from SIRT1 constitutive knockout (KO) mouse brain tissue[8], which yielded a dramatically reduced pull-down of the R3 and R7 fragments (Fig. 3b). To determine the transcriptional modulating activities of these sites, we cloned R3, R7 and the control R5 fragment upstream of a minimal promoter in a pCL3-promoter luciferase reporter construct. Interestingly, co-expression of SIRT1 with reporter constructs containing either R3 or R7, but not R5, significantly reduced, whereas SIRT1 shRNA increased, the expression of the luciferase reporter (Fig. 3c). Collectively, these results indicate that SIRT1 inhibits miR-134 expression by binding directly to distal inhibitory elements.

To verify the contribution of miR-134 to the modulation of CREB by SIRT1, we created SIRT1 loss-of-function in CAD cells by either short hairpin RNA-mediated knockdown (shRNA-SIRT1) or overexpression of a catalytically-inactive mutant of SIRT1(H363Y)[22], both of which elevated the level of miR-134 in these cells (Fig. 3d). The loss of SIRT1 markedly inhibited CREB activity, but this effect was reversed by the administration of LNA-miR-134 (Fig. 3e). These results provide strong evidence that SIRT1 loss-of-function attenuates CREB activity via a miR-134-mediated post-transcriptional mechanism. We searched the R3 and R7 regions for transcription factor consensus binding motifs and discovered Yin Yang 1 (YY1) binding sites within both the R3 and R7 fragments (Fig. 3f, top), but not in any of the other fragments upstream of the miR-134 coding region. YY1 is a ubiquitous and highly conserved transcription factor that can activate or repress gene expression, depending on the cellular context[23]. To determine if YY1 binds to miR-134 regulatory sequences, we performed ChIP experiments using anti-YY1 and anti-SIRT1 antibodies after both overexpression and knockdown of *YY1* in CAD cells. The anti-YY1 antibody immunoprecipitated the R3 and R7, but not the R5, fragments, indicating an association of YY1 with DNA elements within these fragments (Fig. 3f). The knockdown of *YY1* also reduced YY1 binding to the R3 and R7 miR-134 promoter regions in cultured CAD cells (Fig. 3f, lower left). Moreover, the binding of SIRT1 to R3 and R7 was impaired after *YY1* knockdown (Fig. 3f, lower right), indicating that SIRT1 cooperates with YY1 in binding to the upstream regulatory elements of miR-134. Consistent with this idea, in SIRT1 constitutive KO mice, YY1 binding to R3 and R7 of miR-134 was also reduced (Fig. 3g). To determine the functional consequence of YY1 binding to R3 and R7, we used the pCL3-promoter luciferase reporter constructs containing R3, R5 or R7, as described in Fig. 3c. We found that YY1 overexpression repressed, whereas *YY1* knockdown potentiated, the luciferase activity driven by R3 and R7 (Fig. 3h). Conversely, YY1 abundance had no influence on the luciferase activity driven by R5. These results indicate that the binding of YY1 to R3 and R7 represses transcription. We then investigated the influence of YY1 on miR-134 and CREB protein abundance in CAD cells, finding that

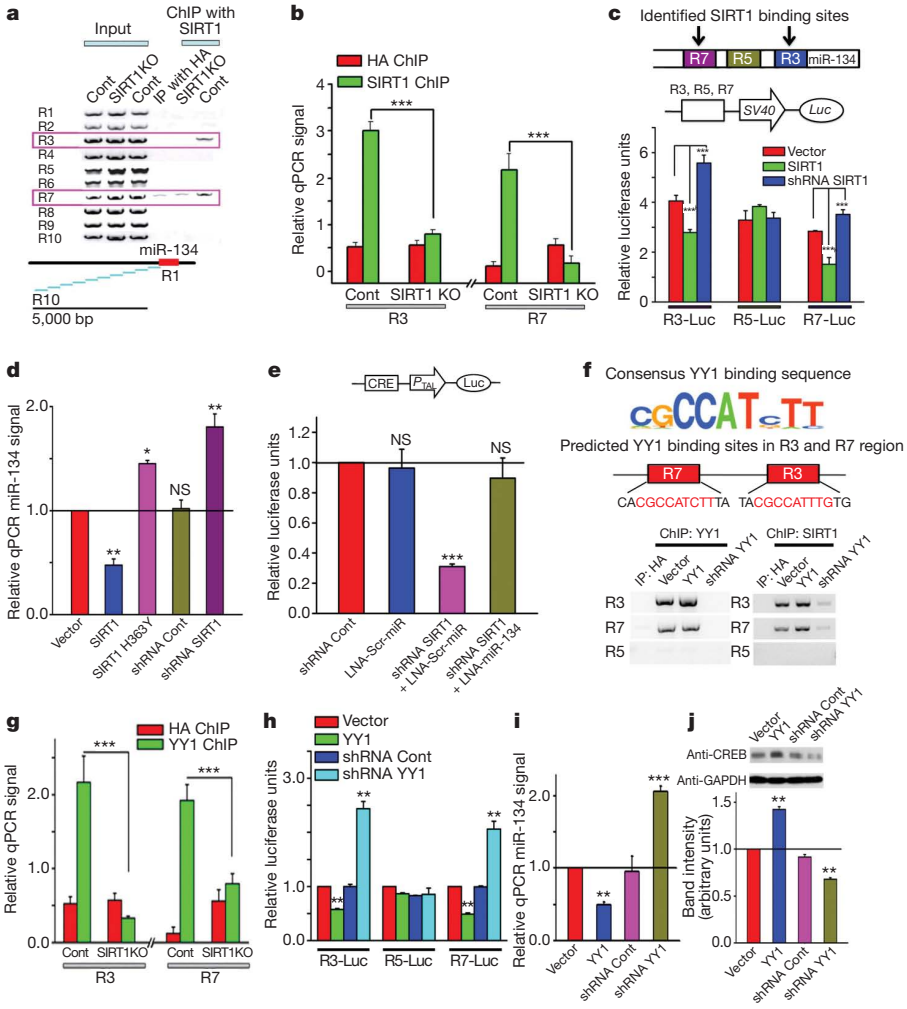

Figure 3 | SIRT1 regulates CREB through miR-134. **a**, From SIRT1 ChIP, two genomic regions, R3 and R7, corresponding to base pairs 1418–830 and 3427–2901 upstream of miR-134, respectively, were amplified from the wild type, but not the SIRT1 total knockout (SIRT1KO), brain tissue. HA, haemagglutinin. **b**, miR-134 promoter regions R3 and R7 were quantified from SIRT1 ChIP with qPCR. **c**, Reporter constructs containing R3, R5 or R7 regions upstream of a minimal promoter in a luciferase reporter were co-transfected with SIRT1, SIRT1 shRNA, or empty vector. **d**, qPCR for miR-134 in CAD cells after transfection with the indicated plasmids. **e**, CRE-luciferase reporter assay in CAD cells. **f**, ChIP was performed on extracts from CAD cells with anti-YY1 and anti-SIRT1 antibodies. **g**, Anti-YY1 ChIP followed by qPCR for regions R3 and R7. **h**, Luciferase reporter constructs containing R3, R5 or R7 regions were co-transfected with the indicated plasmids. **i**, miR-134 levels were measured in CAD cells with qPCR after transfection with the indicated plasmids. **j**, Western blotting measured CREB protein levels in CAD cells after transfections with the indicated plasmids. shRNA Cont, scrambled shRNA control. $*P < 0.05$; $**P < 0.01$; $***P < 0.001$; NS, not significant. All histograms represent average ± s.e.m.

overexpression of YY1 reduced miR-134 expression, whereas miR-134 abundance was increased following the shRNA-mediated knockdown of *YY1* (Fig. 3i). Furthermore, CREB levels were positively regulated by YY1 expression (Fig. 3j). Collectively, these observations support the concept that SIRT1 is recruited to YY1 DNA-binding elements and that the two proteins collaborate to suppress miR-134 expression.

We next examined the role of miR-134 in synaptic plasticity and memory formation. miR-134 was overexpressed in area CA1 of the hippocampus via lentiviral-mediated delivery (Supplementary Fig. 7a). As observed in SIRT1Δ mice, overexpression of miR-134 abrogated LTP in CA1 neurons (Fig. 4a), while basal synaptic transmission was not impaired (Supplementary Fig. 7b). miR-134 overexpression in area CA1 also resulted in a significant impairment in long-term memory formation in the contextual fear-conditioning paradigm (Fig. 4b), but not in the tone-dependent fear conditioning paradigm (Supplementary Fig. 7c), a task reliant upon amygdalar function[24]. miR-134 overexpression did not affect shock sensitivity (Supplementary Fig. 7d). Thus, miR-134 overexpression in the hippocampus closely mimics the effects of SIRT1 loss. These data demonstrate that the upregulation of miR-134 has a role in the synaptic plasticity impairment observed in SIRT1Δ mice.

To assess, *in vivo*, whether miR-134 upregulation underlies the impairment of LTP observed in SIRT1Δ mice, we examined the effect of miR-134 knockdown using injections of the LNA-miR-134 probe into hippocampal CA1 region (Supplementary Figs 8a, b). We found that knockdown of miR-134 restored LTP in acute hippocampal slices from SIRT1Δ hippocampi (Fig. 4c), whereas the LNA probe containing a scrambled sequence (LNA-scr-miR) failed to ameliorate the LTP defects in SIRT1Δ mice. Moreover, injections of LNA-miR-134, but not LNA-scr-miR, into SIRT1Δ mouse hippocampus markedly rescued contextual (Fig. 4d), but not tone-dependent (Supplementary Fig. 8c), fear memory formation. All groups exhibited normal shock sensitivity (Supplementary Fig. 8d). Examination of hippocampal lysates harvested from control and SIRT1Δ mice injected with LNA-scr-miR revealed that both CREB and BDNF protein levels were reduced in SIRT1Δ mice (Fig. 4e). However, LNA-miR-134 treatment restored CREB and BDNF protein to levels comparable to control mice (Fig. 4e).

Our data indicate that the impairments in memory and synaptic plasticity observed in SIRT1Δ mice are, at least, partly mediated via an upregulation of miR-134 and consequent translational inhibition of miR-134 target genes. SIRT1 normally functions in cooperation with YY1, and potentially additional proteins, to restrict the expression of miR-134 and that, upon SIRT1 loss-of-function, higher levels of miR-134 negatively regulate synaptic plasticity via the translational block of key plasticity proteins such as CREB (Supplementary Fig. 1), which subsequently mediates the various synaptic plasticity impairments observed following SIRT1 loss-of-function.

We demonstrated previously that SIRT1 promotes neuronal survival in age-dependent neurodegenerative disorders[5]. We have now found that SIRT1 activity also promotes plasticity and memory in a direct manner through a mechanism distinct from its established neuroprotective activity. This result demonstrates a multi-faceted role of SIRT1 in the brain, further highlighting its potential as a target for the treatment of neurodegeneration and conditions with impaired cognition, with implications for a wider range of central nervous system disorders.

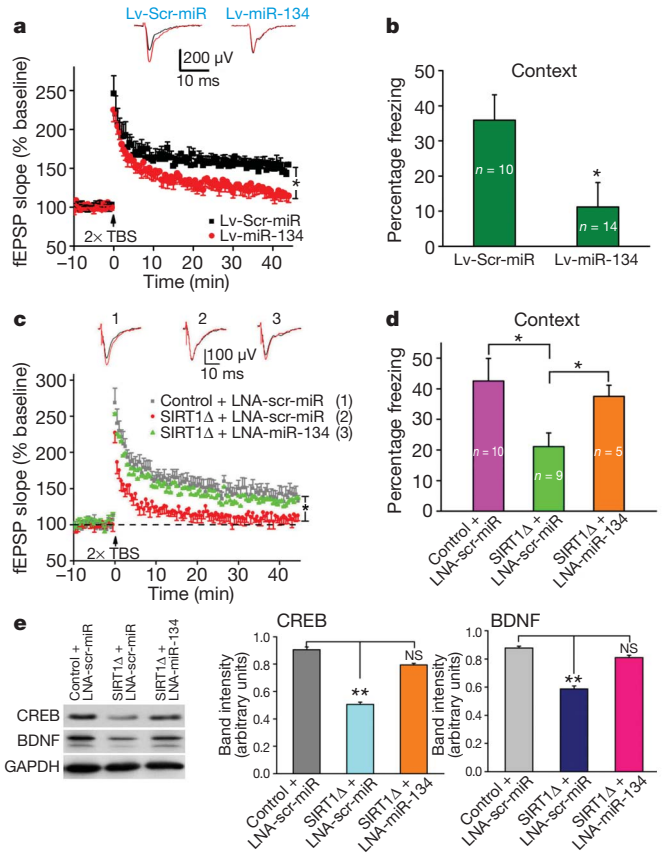

Figure 4 | miR-134 knockdown rescues the LTP and memory impairments caused by SIRT1 deficiency. **a**, LTP was measured in acute hippocampal slices of mice 6 weeks after injection with Lv-miR-134 or Lv-Scr-miR. **b**, Lv-miR-134- and Lv-Scr-miR-injected mice were tested with a contextual fear conditioning task. **c**, Following hippocampal injections with LNA-miR-134 or LNA-scr-miR, LTP was measured in SIRT1Δ and control mouse acute hippocampal slices. **d**, Freezing behaviour in the contextual fear conditioning task was examined in SIRT1Δ and control mice after hippocampal injections of LNA-miR-134 or LNA-scr-miR. **e**, Western blot for CREB and BDNF in brain lysate after *in vivo* miR-134 knockdown. Lv-Scr-miR, control scrambled miR lentivirus. $^{**}P < 0.01$; NS, not significant.

METHODS SUMMARY

For detailed methods, please see the Supplementary Information. The SIRT1 KO and *SIRT1*$^{\Delta ex4}$/*Nestin-Cre* mice were provided by the laboratory of L. Guarente. The plasmids and LNA-miRNA (Ambion) were transfected into mouse CAD cells using Lipofectamine 2000 (Invitrogen) according to the manufacturer's instructions. RNA extraction, purification, and quantitative PCR were performed according to the manufacturer's protocols. Tissue and cell lysis, protein concentrations and western blot analyses were prepared as described previously[5]. Immunoblot data were quantified by measuring the band intensity with NIH imaging software and UN-SCAN-it gel digitizing software (Silk Scientific). Immunostaining was performed as described previously[25] with LSMeta10 software and a confocal microscope (Zeiss). All behavioural testing was performed as described previously[5] and elsewhere. The data were analysed by unpaired Student's *t*-test. Two-way ANOVA was used to compare differences between groups at several time points.

Full Methods and any associated references are available in the online version of the paper at www.nature.com/nature.

Received 28 April; accepted 23 June 2010.
Published online 11 July 2010.

1. Finkel, T., Deng, C. X. & Mostoslavsky, R. Recent progress in the biology and physiology of sirtuins. *Nature* **460,** 587–591 (2009).
2. Kaeberlein, M., McVey, M. & Guarente, L. The SIR2/3/4 complex and SIR2 alone promote longevity in *Saccharomyces cerevisiae* by two different mechanisms. *Genes Dev.* **13,** 2570–2580 (1999).
3. Nakahata, Y. *et al.* The NAD$^+$-dependent deacetylase SIRT1 modulates CLOCK-mediated chromatin remodeling and circadian control. *Cell* **134,** 329–340 (2008).
4. Nakahata, Y., Sahar, S., Astarita, G., Kaluzova, M. & Sassone-Corsi, P. Circadian control of the NAD$^+$ salvage pathway by CLOCK-SIRT1. *Science* **324,** 654–657 (2009).
5. Kim, D. *et al.* SIRT1 deacetylase protects against neurodegeneration in models for Alzheimer's disease and amyotrophic lateral sclerosis. *EMBO J.* **26,** 3169–3179 (2007).
6. Renthal, W. *et al.* Genome-wide analysis of chromatin regulation by cocaine reveals a role for sirtuins. *Neuron* **62,** 335–348 (2009).
7. Cohen, D. E., Supinski, A. M., Bonkowski, M. S., Donmez, G. & Guarente, L. P. Neuronal SIRT1 regulates endocrine and behavioral responses to calorie restriction. *Genes Dev.* **23,** 2812–2817 (2009).
8. Cheng, H. L. *et al.* Developmental defects and p53 hyperacetylation in Sir2 homolog (SIRT1)-deficient mice. *Proc. Natl Acad. Sci. USA* **100,** 10794–10799 (2003).
9. Broadbent, N. J., Squire, L. R. & Clark, R. E. Spatial memory, recognition memory, and the hippocampus. *Proc. Natl Acad. Sci. USA* **101,** 14515–14520 (2004).
10. Calhoun, M. E. *et al.* Comparative evaluation of synaptophysin-based methods for quantification of synapses. *J. Neurocytol.* **25,** 821–828 (1996).
11. Kang, H. & Schuman, E. M. Long-lasting neurotrophin-induced enhancement of synaptic transmission in the adult hippocampus. *Science* **267,** 1658–1662 (1995).
12. Frank, D. A. & Greenberg, M. E. CREB: a mediator of long-term memory from mollusks to mammals. *Cell* **79,** 5–8 (1994).
13. Flavell, S. W. & Greenberg, M. E. Signaling mechanisms linking neuronal activity to gene expression and plasticity of the nervous system. *Annu. Rev. Neurosci.* **31,** 563–590 (2008).
14. Tao, X., Finkbeiner, S., Arnold, D. B., Shaywitz, A. J. & Greenberg, M. E. Ca^{2+} influx regulates BDNF transcription by a CREB family transcription factor-dependent mechanism. *Neuron* **20,** 709–726 (1998).
15. Hong, E. J., McCord, A. E. & Greenberg, M. E. A biological function for the neuronal activity-dependent component of *Bdnf* transcription in the development of cortical inhibition. *Neuron* **60,** 610–624 (2008).
16. Timmusk, T. *et al.* Multiple promoters direct tissue-specific expression of the rat BDNF gene. *Neuron* **10,** 475–489 (1993).
17. Chiaruttini, C., Sonego, M., Baj, G., Simonato, M. & Tongiorgi, E. BDNF mRNA splice variants display activity-dependent targeting to distinct hippocampal laminae. *Mol. Cell. Neurosci.* **37,** 11–19 (2008).
18. Bartel, D. P. MicroRNAs: target recognition and regulatory functions. *Cell* **136,** 215–233 (2009).
19. Fiore, R., Siegel, G. & Schratt, G. MicroRNA function in neuronal development, plasticity and disease. *Biochim. Biophys. Acta* **1779,** 471–478 (2008).
20. Bushati, N. & Cohen, S. M. MicroRNAs in neurodegeneration. *Curr. Opin. Neurobiol.* **18,** 292–296 (2008).
21. Schratt, G. M. *et al.* A brain-specific microRNA regulates dendritic spine development. *Nature* **439,** 283–289 (2006).
22. van der Veer, E. *et al.* Extension of human cell lifespan by nicotinamide phosphoribosyltransferase. *J. Biol. Chem.* **282,** 10841–10845 (2007).
23. Shi, Y., Lee, J. S. & Galvin, K. M. Everything you have ever wanted to know about Yin Yang 1. *Biochim. Biophys. Acta* **1332,** F49–F66 (1997).
24. Fanselow, M. S. & Gale, G. D. The amygdala, fear, and memory. *Ann. NY Acad. Sci.* **985,** 125–134 (2003).
25. Fischer, A., Sananbenesi, F., Wang, X., Dobbin, M. & Tsai, L. H. Recovery of learning and memory is associated with chromatin remodelling. *Nature* **447,** 178–182 (2007).

Supplementary Information is linked to the online version of the paper at www.nature.com/nature.

Acknowledgements We thank R. Jaenisch and M. Rios for providing BDNF knockout frozen brains, L. Guarente and D. Cohen for providing SIRT1Δ and SIRT1 knockout mice, Y. Shi for providing the plasmids expressing YY1 and *YY1* shRNA, A. Mungenast for manuscript editing, K. Singh and M. Dobbin for critical reading of the manuscript, M. Dobbin for help with Supplementary Fig. 5, X. Ge for help with model illustration, and N. Joseph for help with mouse colony maintenance. This work is partially supported by an NIH grant, PO1 AG027916, to L.-H.T.; W.-Y.W. is supported by a Postdoctoral Fellowship from the Simons Foundation; J.Gr. is supported by a Prospective Researchers Fellowship from the Swiss National Science Foundation; J.Gao is supported by the Howard Hughes Medical Institute. L.-H.T. is an investigator of the Howard Hughes Medical Institute.

Author Contributions L.-H.T. designed, directed and coordinated the project. J.Gao designed and performed electrophysiological recordings, behaviour tests, biochemical assays and morphological analyses; W.-Y.W. contributed to the design and generation of microRNA constructs, and performed viral injections, behaviour tests and biochemical analyses; Y.-W.M., J.Gao and L.P. performed luciferase assays and biochemical analyses; J.Gr. and G.M. performed behaviour tests; S.C.S. contributed to viral injection; D.K. contributed to SIRT1 plasmid construction. The manuscript was written by J.Gao, D.K., S.C.S., W.-Y.W. and L.-H.T. and commented on by all the authors.

Author Information The GEO accession number for our microRNA array data is GSE22530. Reprints and permissions information is available at www.nature.com/reprints. The authors declare no competing financial interests. Readers are welcome to comment on the online version of this article at www.nature.com/nature. Correspondence and requests for materials should be addressed to L.-H.T. (lhtsai@mit.edu).

METHODS

Mice. The *SIRT1*$^{\Delta ex4}$/*Nestin-Cre* mice and the *SIRT1* knockout mice were provided by L. Guarente[26]. Floxed littermate mice were used as controls.

Electrophysiological analysis. Electrophysiological analysis was performed as described previously[27]. Transverse hippocampal slices (400-μm thick) were prepared from 5–6-month-old male SIRTΔ or control floxed littermate mice. After decapitation, the brain was rapidly removed and placed in oxygenated (95% O_2/5% CO_2) artificial cerebrospinal fluid (ACSF) at 4 °C. Slices were cut with a Leica VT1000S vibratome (Leica) and maintained at 32 °C for 1 h in a holding chamber filled with oxygenated ACSF. After an equilibration period of at least 2 h at room temperature, a single slice was transferred to the recording chamber, where it was held between two nylon nets and continuously perfused with oxygenated ACSF (23–25 °C) at a flow rate of 2.5–3 ml min^{-1}. The ACSF used for cutting contained (in mM): 75 sucrose, 87 NaCl, 2.5 KCL, 1.25 NaH_2PO_4, 21.4 $NaHCO_3$, 0.5 $CaCl_2$, 7 $MgCl_2$, 1.3 ascorbic acid and 20 D-glucose. The same ACSF was used for both incubation and recording, and contained (in mM): 119 NaCl, 2.5 KCl, 2.5 $CaCl_2$, 1 NaH_2PO4, 1.3 $MgSO_4$, 26.2 $NaHCO_3$ and 11 D-glucose, saturated with 95% O_2/5% CO_2 (pH 7.4). The osmolarity of the ACSF was adjusted to 310–320 mosmol l^{-1}.

For extracellular recordings in the CA1 region of the hippocampus, a bipolar platinum–iridium stimulating electrode was placed in the Schaffer collateral axons to elicit field population responses. The field excitatory postsynaptic potentials (fEPSP) were recorded via a glass micropipette filled with ACSF (1–3 MΩ) placed in the stratum radiatum. Stimuli (0.1 ms duration) were delivered every 30 s. Data were acquired using a HEKA EPC 10 amplifier and analysed by Patchmaster software (HEKA). Peak stimulation-induced fEPSP amplitudes were required to be at least 0.7 mV, and stimulus intensity was set to produce 30–50% of the maximal response. Baseline responses were recorded for 30 min. Theta-burst stimulation (TBS) was delivered as four trains of four pulses at 100 Hz separated by 200 ms and, for the 2× TBS stimulus, repeated twice at 20 s intervals.

Golgi impregnation. Golgi staining was performed as described[28]. Golgi-Cox-stained brains were cut into 200-μm thick sections with a vibratome and analysed using a Zeiss 200 Axiovert microscope and Openlab software. The number of apical and basal spines on hippocampal CA1 pyramidal neurons was counted blind to the genotype. For each experimental group, a minimum of ten cells per slice (animal number $n = 3$) was analysed. CA1 hippocampal neurons within the region −1.4 mm to −1.6 mm (relative to Bregma) were included for the analysis.

Immunohistochemistry. Immunohistochemical analysis was performed as described[25]. The anti-synaptophysin (SVP-38) antibodies (Sigma) were used at a 1:1,000 concentration. Confocal images stacks ($z = 1$ μm) were scanned. LSMeta10 software (Zeiss) was used to calculate the mean synaptophysin intensity. Brain sections with the strongest fluorescent intensity were scanned first. Subsequent images included in the analysis were scanned using the same settings. SVP immunofluorescence was quantified using LSMeta10 software (Zeiss).

Protein extraction and immunoblotting. Hippocampi were collected and lysed in RIPA buffer. The lysates were incubated for 15 min on ice, centrifuged for 15 min at 4,000*g* at 4 °C, and supernatant was collected. The lysates were subjected to 10% SDS–PAGE followed by immunoblotting.

Chromatin immunoprecipitation (ChIP). ChIP was performed as described[27]. Briefly, brains were chemically cross-linked by the addition of one-tenth volume of fresh 11% formaldehyde solution for 15 min at room temperature, homogenized, resuspended, lysed in lysis buffer, and sonicated to solubilize and shear crosslinked DNA. We used a Misonix Sonicator 3000 and sonicated at power 7 for 10 × 30 s pulses (90 s pause between pulses) at 4 °C while samples were immersed in an ice bath. The resulting whole-cell extract was incubated overnight at 4 °C with 100 μl of Dynal Protein G magnetic beads that had been pre-incubated with 10 μg of the appropriate antibody. Beads were washed five times with RIPA buffer and once with TE buffer containing 50 mM NaCl. Bound complexes were eluted from the beads by heating at 65 °C with occasional vortexing and crosslinking was reversed by overnight incubation at 65 °C. Whole-cell DNA extract (reserved from the sonication step) was also treated for cross-link reversal. Immunoprecipitated DNA and whole-cell DNA were then purified by treatment with RNase A, proteinase K, and multiple phenol:chloroform:isoamyl alcohol extractions. Purified DNA samples were normalized and subjected to PCR analysis. The antibodies used for ChIP were anti-Sir2 and anti-CREB from Abcam. After immunoprecipitation, recovered chromatin fragments were subjected to quantitative real-time PCR or semiquantitative PCR for 32–40 cycles using primer pairs specific for 250–500 bp segments corresponding to mouse gene promoter regions.

RNA extraction and reverse transcription. RNA was extracted with TRIzol (Invitrogen) using a homogenizer according to the manufacturer's protocol. RNA quality was assessed using the Lab-on-a-Chip 2100 Bioanalyzer (Agilent) platform. Standard gene expression TaqMan assays were purchased from Applied Biosystems and performed according to the manufacturer's protocol. For gene expression analysis, 0.1–1 μg of RNA was DNase I-treated (Promega) and reverse- transcribed using 250 ng of random primers and SuperScript III (Invitrogen) according to the manufacturer's protocol. For mRNA analysis, data were normalized using *GAPDH*. For miR TaqMan, data were normalized using miR-202.

Real-time PCR. Real-time PCR was carried out with SYBR-Green-based reagents (Invitrogen, express SYBR GreenER) using a CFX96 real-time PCR Detection system (Bio-Rad). The relative quantities of immunoprecipitated DNA fragments were calculated using the comparative C_T method. Results were compared to a standard curve generated by serial dilutions of input DNA. Data were derived from three independent amplifications. Error bars represent standard deviations.

Primer sequences used for PCR. BDNF; 5′-ATGGGACTCTGGAGAGCCTGAA-3′, 5′-CGCCAGCCAATTCTCTTTTTGC-3′. BDNF PI; 5′-TGATCATCACTCACGACCACG-3′, 5′-CAGCCTCTCTGAGCCAGTTACG-3′. BDNF PII; 5′-TGAGGATAGTGGTGGAGTTG-3′, 5′-TAACCTTTTCCTCCTCC-3′. BDNF PIV; 5′-GCGCGGAATTCTGATTCTGGTAAT-3′, 5′-GAGAGGGCTCCACGCTGCCTTGACG-3′. CREB; 5′-TCAGCCGGGTACTACCATTC-3′, 5′-TTCAGCAGGCTGTGTAGGAA-3′. GAPDH; 5′-TTGTTGCCATCAACGACCCC-3′, 5′-ATGAGCCCTTCCACAATGCC-3′.

Cell cultures and transient transfection. CAD cells were grown in DMEM/F12 medium supplemented with 8% fetal bovine serum at 37 °C and 5% CO_2. Cells were transiently transfected with equal molar amounts of the various luciferase-fusion constructs or the pGL3-basic construct in serum-free growth media using Lipofectamine Plus reagent according to the manufacturer's protocol (Invitrogen). pRL-tK (Promega) containing the *Renilla* luciferase gene was cotransfected for the normalization of transfection efficiencies. For experiments that examined the effects of exogenously expressed $shRNA_{SIRT1}$, Sirt1(H363Y), YY1, $shRNA_{YY1}$, miR-134 or scrambled miR controls, luciferase-fusion reporter constructs and pRL-tK were co-transfected. After 3 h incubation with the DNA/Lipofectamine Plus complexes, the cells were incubated in fresh media containing serum. Transfected cells were lysed 48 h after transfection and luciferase activity was determined using the dual-luciferase reporter assay system (Promega).

Taqman miRNA real-time qPCR. Total small RNA was extracted using the PureLinK miRNA isolation kit (Invitrogen) according to the manufacturer's instructions with minor modifications. RNA was reverse-transcribed using specific miRNA stem-loop primers and the Taqman microRNA reverse transcription kit (Applied Biosystems). Mature miRNA expression was measured with Taqman microRNA assays (Applied Biosystems) according to the manufacturer's instructions. The expression of each miRNA was normalized against the expression level of the small nucleolar RNA snoRNA202, and presented as the mean normalized expression. Putative mRNA targets for miRNAs were predicted using the computer programs Targetscan, PicTar and miRanda.

Microarray. Total RNA from the hippocampus of SIRT1Δ mice and floxed controls was isolated with TRIzol reagent (Invitrogen) according to manufacturer's instructions, and purified using Qiagen's RNA Cleanup kit. Ten micrograms of glycogen (Ambion) was added as a carrier before precipitation. The microarray experiment was carried out by Exiqon. Briefly, LNA-modified oligonucleotide probes for all mouse microRNAs annotated in miRBase version 7.1 were used for screening control and SIRT1Δ hippocampal RNA. More information is available at http://www.exiqon.com.

Construction of expression plasmids. All constructs were produced using standard molecular methods and confirmed by DNA sequencing. Mouse miR-134 was amplified from mouse genome library using the primers 5′-ACTGCAGCCAACCTTGGTGAGGCAGCTG-3′ and 5′-ATGCTAGCCTCGAGTCCTGGTCCACTGAGCAGGC3′, and cloned into the lentiviral expression vector Lv-CMV-WPRE. All microRNAs were cloned the same way into the same vector. For *in vivo* overexpression of miR-134, the cytomegalovirus promoter was replaced with the PGK promoter and miR-134 or the scrambled miR sequences were added to produce LV-miRNA-134 and LV-Scr-miRNA.

The luciferase reporter vector pGL3-promoter (Promega) was used as the backbone for the luciferase reporter plasmids pGL3p-R3, pGL3p-R5 and pGL3p-R7. The DNA fragments R3, R5 and R7 were amplified from mouse genomic DNA and inserted upstream of the minimal SV40 promoter. The primers used were for R3, 5′-ATGGTACCTGAATGATTCGGTGGGCTGC-3′ and 5′-TCAGATCTATCCCAGGTGATCCTCCACTC-3′; for R5, 5′-ATGGTACCGGAAGACTTGCTGCATGGTGG-3′ and 5′-TCAGATCTTTCCCACTATGAAGCAAGACAG-3′; for R7, 5′-ATGGTACCTCACTGAGGTCCTGTCCCTG-3′ and 5′-TCAGATCTCTCTGGCAAAGAGAGGAAGC-3′.

The pRLTK-3CREB and pRLTK-3mutCREB plasmids were cloned as described[29]. Briefly, the CREB 3′UTR fragment including three miR-134 target sequences was amplified from the mouse genome and inserted into the 3′UTR of

a luciferase reporter gene. To mutate the miR-134 binding sites in the *CREB* 3′UTR, five mutations were made in each target sequence using overlapping PCR. The mutated miR-134 target sequence in the *CREB* 3′UTR are as follows GUUACCAGUCACUUA, AAGUUAACAGUCACU and UUUUGCAUUAAA CUG.

Fear conditioning tests. Context-dependent fear conditioning training consisted of a 3 min exposure of mice to the conditioning box (context) followed by a foot shock (2 s, 0.8 mA, constant current). The memory test was performed 24 h later by re-introducing the mice into the conditioning context for 3 min. Freezing, defined as a lack of movement, except for breathing, associated with a crouching posture, was recorded every 10 s by two trained observers (one was unaware of the experimental conditions) during 3 min (a total of 18 sampling intervals). The number of observations indicating freezing obtained as a mean from both observers was expressed as a percentage of the total number of observations.

Tone-dependent fear conditioning training consisted of a 3-min exposure of mice to the conditioning box, followed by a tone (30 s, 20 kHz, 75 dB sound pressure level) and a foot shock (2 s, 0.8 mA, constant current). The memory test was performed 24 h later by exposing the mice for 3 min to a novel context followed by an additional 3 min exposure to a tone (10 kHz, 75 dB sound pressure level). Freezing was recorded every 10 s by two nonbiased observers as described above.

Morris water maze test. The water maze hidden platform paradigm[30] was performed in a circular tank (diameter 1.8 m) filled with opaque water. A platform (11×11 cm) was submerged below the water's surface in the centre of the target quadrant. The swimming path of the mice was recorded by a video camera and analysed by the Videomot 2 software (TSE). For each training session, the mice were placed into the maze consecutively from four random points of the tank. Mice were allowed to search for the platform for 60 s. If the mice did not find the platform within 60 s, they were gently guided to it. Mice were allowed to remain on the platform for 15 s. Three training trials were given every day; the latency for each trial was recorded for analysis. During the memory test (probe test), the platform was removed from the tank, and the mice were allowed to swim in the maze for 60 s.

Novel object recognition. The novel object recognition test was performed as described elsewhere[31], with the following modifications. Before training, mice were habituated to the open testing arena ($41.3 \times 41.3 \times 30.5$ cm) over 2 days, for four trials per day, each lasting 5 min. During training, mice were exposed to three unknown objects that they were allowed to explore during four sessions of 5 min each. The objects had previously been put into a dirty cage to avoid olfactory preferences. Object memory was tested 1 day later by replacing one of the objects with a novel one and measuring the time with which the animals explored the novel object during a 10-min exploration session. The location of the object was counterbalanced between mice. Object exploration was scored by an automated software (Ethovision XT) and expressed by a discrimination index $DI = (t_{\mathrm{novel}} - (t_{\mathrm{familiar1}} + t_{\mathrm{familiar2}})/t_{\mathrm{total}})$ with t_{novel} and t_{familiar} being the time spent with the novel and the familiar object, respectively, and t_{total} being the total time spent with all objects.

Cannulation and injections. Double cannulae (Plastic1) were implanted 7 days before the experiments, under anaesthesia. For scrambled miR lentivirus, miR-134 lentivirus, fluorescently-labelled LNA-scrambled-miR, or LNA-anti-miR-134 (Exqion) injections, cannulae were placed in the dorsal hippocampus, antero-posterior −1.5 mm, lateral 1 mm, depth 2 mm. Solution (1.5 µl) was injected as described above into the bilateral hippocampus. Scrambled miR or miR-134 lentivirus was injected once. For LTP recording, fluorescently labelled LNA-scrambled-miR or LNA-anti-miR-134 was injected once, whereas for the behavioural tests, LNA probes were injected three times, once every 2 days.

26. Cohen, D. E., Supinski, A. M., Bonkowski, M. S., Donmez, G. & Guarente, L. P. Neuronal SIRT1 regulates endocrine and behavioral responses to calorie restriction. *Genes Dev.* **23,** 2812–2817 (2009).
27. Guan, J. S. *et al.* HDAC2 negatively regulates memory formation and synaptic plasticity. *Nature* **459,** 55–60 (2009).
28. Fischer, A., Sananbenesi, F., Pang, P. T., Lu, B. & Tsai, L. H. Opposing roles of transient and prolonged expression of p25 in synaptic plasticity and hippocampus-dependent memory. *Neuron* **48,** 825–838 (2005).
29. Doench, J. G. & Sharp, P. A. Specificity of microRNA target selection in translational repression. *Genes Dev.* **18,** 504–511 (2004).
30. Morris, R. G., Garrud, P., Rawlins, J. N. & O'Keefe, J. Place navigation impaired in rats with hippocampal lesions. *Nature* **297,** 681–683 (1982).
31. Stefanko, D. P., Barrett, R. M., Ly, A. R., Reolon, G. K. & Wood, M. A. Modulation of long-term memory for object recognition via HDAC inhibition. *Proc. Natl Acad. Sci. USA* **106,** 9447–9452 (2009).